Published in final edited form as:
Chem Res Toxicol. 2009 March 16; 22(3): 526–535. doi:10.1021/tx800402y.

Mechanistic Aspects of the Formation of Guanidinohydantoin from Spiroiminodihydantoin under Acidic Conditions

Yu Ye[‡,§], **Barbara H. Munk**[†,§], **James G. Muller**[‡], **Alexander Cogbill**[‡], **Cynthia J. Burrows**[‡], and **H. Bernhard Schlegel**[†,*]

[†]Department of Chemistry, Wayne State University, Detroit, Michigan, 48202

[‡]Department of Chemistry, University of Utah, 315 S. 1400 East, Salt Lake City, Utah 84112

Abstract

Experimentally, it was observed that the oxidized guanine lesion spiroiminodihydantoin (Sp) contained in highly purified oligodeoxynucleotides slowly converts to guanidinohydantoin (Gh). The reaction is accelerated in the presence of acid. The possible mechanisms of this transformation have been analyzed computationally. Specifically, the potential energy surface for formation of Gh from Sp has been mapped using B3LYP density functional theory, the aug-cc-pVTZ and 6-31+G(d,p) basis sets and the IEF-polarizable continuum model (PCM) solvation model. The results favor a mechanism in which proton-assisted hydration of the C6 carbonyl group forming a gem-diol leads to ring opening of the iminohydantoin ring. The resulting species resembles a β-ketoacid in its ability to decarboxylate; tautomerization of the resulting enol forms Gh. The results of these studies indicate that incubation of nucleosides or oligonucleotides containing Sp should be avoided in acidic media when high purity or an accurate assessment of the amounts of hydantoin lesions is desired.

Introduction

Spiroiminodihydantoin (Sp, **1**) and guanidinohydantoin (Gh, **7**) are secondary oxidation products of the guanine nucleobase with highly mutagenic properties.(1,2) Formation of both of these oxidation products from guanine and 8-oxoguanine has been studied extensively over the last decade. (3-22) Experimental and computational studies have indicated that both Sp and Gh are formed via a common intermediate, 5-hydroxy-8-oxoguanine (5-OH-OG) (Scheme 1). (7,9,10,23) The ratio of Sp to Gh observed in vitro has been shown to be dependent on the pH and temperature of the reaction. High pH and temperature favor the rearrangement of 5-OH-OG to form Sp, **1**, while low pH and temperature favor hydration of 5-OH-OG and subsequent loss of CO_2 to form Gh, **7**.(24)

Similarly, the formation of spirodihydantoin (Scheme 1), a minor product formed during the oxidation of uric acid to allantoin, was also found to be correlated with high pH and temperature.(25) The formation of allantoin via the oxidation of uric acid has been the subject of experimental study for many years.(26,27) Allantoin differs from Gh, **7,** by the substitution of a carbonyl group instead of an imino group at the C2 position. ^{13}C NMR studies provided evidence that the formation of allantoin from 5-hydroxyisourate under basic conditions proceeds via hydrolysis of the N1-C6 bond followed by a 1,2 carboxylate shift and then

*Corresponding author. Tel: (313) 577-2562. Fax: (313) 577-8822 hbs@chem.wayne.edu.
§These authors contributed equally to this work.

Supporting Information Available: The optimized molecular geometries in Cartesian coordinates for all adducts and corresponding transition states, the structures for the tri-O-acetyl-8-oxoG and tri-O-acetyl-Sp, and the analysis of the Sp nucleoside at pH 5.3 are provided in the Supporting Information. This material is available free of charge via the Internet at http://pubs.acs.org.

decarboxylation (Scheme 1).(27) In the latter experiment, the carboxylate shift from the C5 to C4 position was confirmed by preparing [4,6-$^{13}C_2$]urate and following its conversion over time to allantoin via ^{13}C NMR. The signals from the C4 and C6 were doublets with coupling constants consistent with the J_{cc} values observed for the α- and carbonyl carbons in amino acids.

Rather than the carboxylate shift proposed above, these experimental results could also suggest that under basic conditions, formation of allantoin may proceed through a short lived spirodihydantoin intermediate. This alternative mechanism is consistent with the experimental observation that the oxidized guanine lesion spiroiminodihydantoin (Sp) contained in highly purified oligodeoxynucleotides slowly converts to guanidinohydantoin (Gh). As with formation of Sp and Gh from 5-OH-OG, this conversion is sensitive to reaction pH. The present study evaluates the possible formation of Gh directly from Sp via hydration of the carbonyl group at C6 and subsequent loss of carbon dioxide. The effect of pH on the possible mechanisms for this conversion have been evaluated computationally.

Experimental Methods

Synthesis of 2',3',5'-tri-O-acetyl-8-oxo-7,8-dihydroguanosine(7)

A mixture of 7,8-dihydro-8-oxoguanosine (25 mg) and 4-dimethylaminopyridine (2 mg) in acetic anhydride (2.5 mL) was stirred at room temperature for 3 days. To the resulting mixture was added 15 mL toluene, and the solution was evaporated under reduced pressure 4 times. The yield was above 95%. The resulting residue was characterized by ESI-MS mass spectrometry, found to have a purity of >95%, and used without further purification.

Synthesis of 2',3',5'-tri-O-acetyl-spiroiminodihydantoin

To a 1-mL solution of 75 mM potassium phosphate (pH 8.0) and 2',3',5'-tri-*O*-acetyl-8-oxo-7,8-dihydroguanosine (2 mg, 4 mmol) was added Na_2IrCl_6 (4 mg, 8 mmol). The solution was incubated at room temperature for 30 min. The reaction mixture was purified by HPLC with a 4.6 mm × 250 mm Alltima C18-NUC (Alltech) reversed-phase column using an isocratic solvent system consisting of 12% acetonitrile and 88% water (0.1%TFA). The flow rate was 1.0 mL/min, and the UV spectra were recorded at 220 nm.

Analysis of the conversion of spiroiminodihydantoin to guanidinohydantoin under acidic conditions

For nucleoside studies, the purified spiroiminodihydantoin nucleoside triacetate was incubated in HPLC buffer (12% acetonitrile, 88% water and 0.1% TFA, pH=1.5) at room temperature. The incubated spiroiminodihydantoin was then analyzed by LC/MS at different time points over the course of several days. The studies were repeated at pH 2.0, 2.5 and 5.3.

The nucleoside samples were analyzed by positive electrospray ionization (ESI) on a Waters SQ mass spectrometer equipped with a Waters Acquity UPLC system. Chromatographic separation was accomplished using a Waters Acquity UPLC HSS T3 (1.8 μm, 50×2.1mm) reversed phase column and a linear gradient of 5% solvent B to 90% solvent B over 6.5 min. Solvent A consisted of 0.1% formic acid in water, while solvent B was acetonitrile. The flow rate was 0.6 mL/min, and UV spectra were recorded in the range of 210-400 nm. The mass spectrometer source and desolvation temperatures were 150°C and 400°C, respectively. The capillary voltage was set to 3.5 kV, sampling cone voltage to 17 V, and the extractor cone to 3V. The instrument was operated and data accumulated with Micromass Masslynx software (version 4.1). The relative ionization efficiency of Gh:Sp on this instrument was previously found to be 2.4:1,(8) and this factor was used to correct the values reported herein.

For oligomer studies, an Sp-containing 13mer with the sequence 5'-d (CGTCCASpGTCTAC)-3' was prepared by Na_2IrCl_6-mediated oxidation of an OG-containing synthetic oligomer according to previously published methods.(24) Solutions of the oligomer (10 μM) were incubated at pH 3.5 or 4.5 for 5 days at room temperature, and then analyzed by HPLC on a Beckman 126 solvent module equipped with a Beckman 168 PDA detector. Chromatographic separation was accomplished using a Dionex DNAPac PA-100 (250×4.6mm) ion-exchange column with a linear gradient of 15% B to 100% B in 30min. Solvent A was 10% acetonitrile and 90% water, while solvent B was 10% acetonitrile and 90% 1.5 M sodium acetate (pH 7). The flow rate was 1.0mL/min and UV-spectra were recorded at 260nm.

Computational Methods

Molecular orbital calculations were carried out using the development version of the GAUSSIAN series of programs.(28) Optimized geometries and energies in the gas phase were computed with the B3LYP density functional method(29-31) using the 6-31+G(d,p) basis set (32-37) for all but two of the reactants, products and transition states. The transition states for two of the acyl migration reactions (16/23TS and 1N1Htaut/22TS) were located by optimizing the geometries in solution using the IEF-PCM solvation model(23). Our previous computational studies with the 8-hydroxyguanine radical indicated that the potential energy profiles of adducts substituted at N9 with methyl, hydroxymethyl and methoxyethyl were similar to those observed with hydrogen as the substituent.(38) Therefore, the model compounds for the calculations were the Sp and Gh nucleobases with hydrogen as the substituent at N9.

Transition states involving proton transfer from one adduct to another were modeled with one or two explicit molecules of water assisting the proton transfer. In general, the transition states thus formed were six-membered rather than four-membered ring systems and should therefore represent a lower energy pathway. For addition of water to the C6 carbonyl, two waters are needed to form the six-membered ring. For proton relays, two waters were usually needed to span the space between the proton donor and the proton acceptor. In a few cases due to the geometry of the intermediate, it was possible to form a six-membered ring transition state with only one water molecule. Addition of a second explicit water molecule to the latter calculations would result in an eight-membered ring transition state and was not thought unlikely to provide a lower energy pathway. Single point calculations in aqueous solution were carried out at the gas phase optimized geometry for the adducts and corresponding transition states using IEF-PCM at the B3LYP/aug-cc-pVTZ(39) level of theory. The computations were conducted with the F01, F02, F02plus and G01 development versions of the Gaussian suite of programs and employed a solvent excluding surface cavity model, UAKS radii, and tesserae with an average area of 0.200 $Å^2$. Cartesian coordinates for the optimized geometries and gas phase energies for the adducts and transition states are provided in the Supporting Information. Vibrational frequencies were computed in the gas phase at the B3LYP level with the 6-31+G(d,p) basis set and were used without scaling since the B3LYP frequencies agree quite well with experimental values for a wide range of second and third period compounds.(40) Thermal corrections and enthalpies were calculated by standard statistical thermodynamic methods (41) using the unscaled B3LYP frequencies and the ideal gas / rigid rotor / harmonic oscillator approximations. The energy in solution for each species is the sum of the electronic energy in the gas phase calculated at B3LYP/aug-cc-pVTZ//B3LYP/6-31+G(d,p), the ZPE and thermal corrections for enthalpy at B3LYP/6-31+G(d,p), and the solvation free energy calculated at IEF-PCM/B3LYP/aug-cc-pVTZ//B3LYP/6-31+G(d,p).

To maintain the charge balance within the calculations, proton transfer between cation adducts was modeled as a proton transfer to guanine's Watson-Crick base pair partner, cytosine

Between anions the charge balance was maintained by assuming the proton is transferred from the neutral adduct to a methane thiol anion and, conversely, from the neutral methane thiol back to an anion adduct. Methane thiol has been selected as the smallest possible model for dithiothreitol, a reagent commonly used experimentally for examining electron and proton transfer within DNA.

Results and Discussion

Experimental analysis

The spirocyclic nucleoside Sp is a major product of oxidation of G or OG under neutral or basic conditions (i.e., pH≥7).(24) We observed that a purified Sp sample stored at pH 1.5 for 24 hrs at room temperature formed trace amounts of Gh (5%). Interestingly, repurification of this Sp sample still gave a trace amount of Gh as the impurity. This puzzling observation led to a hypothesis that Sp is converted to Gh under acidic conditions.

To test this hypothesis, Sp nucleoside (Supporting Information, Figure S-3) was incubated at pH 1.5 at room temperature for 1, 5 and 17 days, and the composition was examined by LC/MS. The results indicated that a significant amount of Gh (~30%) appeared in the sample after 5 days (Figure 1). Since little Gh was detected in a fresh Sp sample, the possibility of a significant amount of Gh originating in mass spectrometry can be ruled out. After 17 days, most of the mixture (~90%) had been converted to Gh (Figure 1). Therefore it can be concluded that Sp converts to Gh at pH 1.5 at room temperature with a half life of approximately 9 days for nucleoside samples.

The conversion of Sp to Gh is highly acid sensitive; the amount of Gh formed after 3 days decreased dramatically if the pH of medium was raised to 2 or 2.5 (Figure 2). To further probe the acid sensitivity, the Sp nucleoside was incubated at pH 5.3 at 37°C overnight; these conditions mimic those used during nuclease digestion with enzymes such as nuclease P1. Under these conditions, no significant increase in the amount of Gh could be detected (see Supporting Information).

Additional studies were performed to examine the conversion of Sp to Gh in an oligodeoxynucleotide. In oligomers shorter than 50mers, the Sp and Gh-containing strands of identical sequence are usually separable by HPLC. Thus, a 13mer sequence 5'-d (CGTCCASpGTCTAC)-3' was incubated at pH 3.5 or 4.5 for 5 days followed by HPLC analysis. Note that prolonged incubation at lower pHs was not carried out due to the possibility of competing depurination reactions in the oligomer that would complicate the analysis. HPLC separation and confirmation of structure by negative ion ESI-MS showed that small but significant amounts of Gh (~5%) were formed in this time period at pH 3.5.

Comparing the structures of Sp and Gh, three steps have to be involved in the mechanism of the Sp to Gh conversion: water addition, ring opening and decarboxylation. The hydantoin ring of Sp may break between C4 and C5 or between C6 and N1 (Scheme 1). Moreover, water addition may occur before or after ring opening. Accordingly three possible pathways are proposed and evaluated by computational methods.

Computational Analysis

Four pathways for conversion of Sp, **1**, to Gh, **7**, were evaluated (Schemes 2-5). In Pathway A, water adds to the carbonyl group at C6 forming a *gem*-diol intermediate (**3, 8**, and **11**) which can undergo ring-opening to a 4-carboxy-guanidinohydantoin (4-carboxy-Gh) intermediate (**4**, **9**, and **12**). Loss of carbon dioxide leads to formation of the Gh-enol (**5**, **10**, and **13**) which then tautomerizes to form Gh, **7**. Pathway B examines the energetics of concerted water addition to C6 and cleavage of the C6-C4 bond to form a carbamate intermediate, **14**. This

intermediate can then lose carbon dioxide and tautomerize to form Gh, **7**. Pathway C begins with cleavage of the C6-C4 bond to form the isocyanate intermediate, **16**. Addition of water to the isocyanate yields the carbamate intermediate, **17**, which loses carbon dioxide and tautomerizes to Gh, **7**. Pathway D outlines the energetics for formation of Gh, **7**, from Sp, **1** via reversion to 5-OH-OG and then acid-catalyzed hydration of the carbonyl at C6 and decarboxylation to Gh.

Pathway A (Scheme 2)—The energetics for formation of Gh, **7**, from Sp, **1**, via the *gem*-diol intermediate have been evaluated for acidic, neutral and basic conditions by conducting the calculations with protonated, neutral and anionic species (Figure 4). For the protonated species, the positive charge in the relative energy calculations is balanced by assuming that the proton moves from a cytosine cation (CH^+) to neutral Sp, **1**. For the hydroxide and other anionic species (e.g., **11**, **12**, and **13**) the calculation assumes that the proton moves from a neutral water molecule or other reaction intermediate to a CH_3S anion.

The various species evaluated for Pathway A are shown in Scheme 2. Relative energies of the reactants, intermediates, and products are provided in Figure 4 and Table 1. Under neutral conditions, addition of water to Sp, **1**, to form the *gem*-diol, **8**, is endothermic by 14.7 kcal/mol with a forward barrier height modeled with one reactive and one catalytic molecule of water of 43.0 kcal/mol. The diol, **8**, can undergo concerted proton transfer and ring opening to form the 4-carboxy-Gh intermediate, **9**. This reaction is predicted to be thermo-neutral with a difference in energy between the two species of -0.2 kcal/mol and a forward barrier height of 16.3 kcal/mol when modeled with one explicit water molecule assisting with the proton transfer. The proton transfer and decarboxylation of **9** yields Gh-enol, **10,** and is predicted to be endothermic by 4.6 kcal/mol with a forward barrier height, modeled with two explicit molecules of water, of 23.1 kcal/mol. The enol-keto tautomerization of **10** to form Gh, **7**, is exothermic by 24.6 kcal/mol. These results agree with the experimental observation that the keto form of small molecules is generally more stable than the corresponding enol form. In the case of acetone, the keto form is 12 to 13.9 kcal/mol lower in energy.(42) The forward barrier height modeled with two molecules of water is 26.1 kcal/mol which is consistent with published calculations for the keto-enol tautomerization of acetone and in line with the experimental observation that the two Gh diasteromers epimerize at room temperature with a half-life of about 30 min.(9) A study conducted by Lee et al.(43) indicates that addition of one catalytic molecule of water lowered the solution phase barrier height from 73.1 (uncatalyzed reaction) to 45.1 kcal/mol (MP2/6-31G(d,p)//MP2/6-31G(d,p) level of theory). Calculations on the keto-enol tautomerization of acetone conducted by Cucinotta et al. using ab initio molecular dynamics provided a similar barrier height for the reaction catalyzed by one molecule of water and suggest that addition of further water molecules may bring the barrier down by a few more kcal/mol.(42) Based upon the experimental findings of Capon et al., under acidic conditions, the rate for the enol/keto tautomerization, may increase by an order of magnitude, suggesting 1.5-3 kcal/mol decrease in the barrier height for this reaction.(44)

Acid-mediated addition of water to the C6 carbonyl of Sp, **1**, is most likely to occur via protonation at the N-1 nitrogen, **2**, and is predicted to be endothermic by 4.1 kcal/mol. Protonation at the oxygen of either the Sp C6 carbonyl or C5 carbonyl is unlikely to occur as these species are predicted to be 23.4 and 13.8 kcal/mol higher in energy, respectively, than **2**. The protonated *gem*-diol formed from **2** is the N-1H protonated Sp-diol, **3**. The forward barrier height for formation of **3** from **2** modeled with two explicit water molecules is 14.5 kcal/mol, 28.5 kcal/mol lower than the barrier height for addition of water to the C6 carbonyl of unprotonated Sp **(1/8 TS)**. Ring-opening of the protonated diol intermediate, **3**, yields 4-carboxy-Gh protonated at N1, **4**. Similar to the unprotonated reaction (**8/9 TS**), this reaction is predicted to be nearly thermo-neutral with a difference in energy between **3** and **4** of 1.0 kcal/mol. However, the forward barrier height for this reaction is 35.1 kcal/mol, 18.8 kcal/mol

higher than the height predicted for the unprotonated species (**8/9 TS**). Reaction path following calculations indicate that **3** to **4** transition begins with nearly complete cleavage of the C6-N1 bond (C6-N1 bond distance ~2Å) prior to transfer of a proton from the gem diol to the already protonated N1 position of the guanidine subunit. In a separate calculation modeled without an explicit water molecule, the transition state for ring-opening of **3** to form a 4-carboxy-Gh intermediate protonated at the C-6 carboxylic acid was estimated to be 48.9 kcal/mol suggesting that the large forward barrier height is being driven by the energy require to cleave the C6-N1 bond. In contrast, the **8** to **9** transition begins with transfer of a proton from the gem diol to an unprotonated N1 position followed by cleavage of the C6-N1 bond. Concurrent ring-opening and proton transfer to form a 4-carboxy-guanidinohydantoin species protonated at the oxygen of the C5 carbonyl was also examined but this intermediate, **4C5OH$^+$ taut**, is 29.5 kcal/mol higher in energy than **4** making it thermodynamically unfavorable.

Results of calculations from a previous computational study(45) suggest that the pK_a of Sp is ~0.5, similar to that observed for 8-oxoguanine (pK_a (exp) = -0.1).(46) At pH 2, approximately 18.5% of the Sp should be protonated (**2**) and this would facilitate formation of the tetrahedral gem diol intermediate (**4**). The pK_a of intermediate **4** is predicted to be 5.6 calculated using the same method as that described in our previous research. At pH 2, 3% of the gem diol intermediate is predicted to be unprotonated and available to proceed via the kinetically preferred transition state (**8/9 TS**). A plot of the predicted percentage of protonated Sp and Sp-diol is provided in the Supporting Information.

The carboxylic acid intermediate, **4**, may undergo decarboxylation to yield a protonated Gh enol, **5**. This reaction is slightly exothermic (1.6 kcal/mol) and is predicted to have a forward barrier height of 22.9 kcal/mol. Enol-keto tautomerization of Gh enol, **5**, provides a protonated Gh, **6**. As expected, the keto form of the protonated Gh, **6**, is 22.4 kcal/mol more stable than the enol form. The forward barrier height for this tautomerization is predicted to be 24.3 kcal/mol. Consistent with experimental data indicating that the pKa of guanidine is 13.8(47), the protonated form of Gh, **6**, is thermodyanically favored over the unprotonated species, **7**.

Formation of the *gem*-diol under basic conditions has been modeled by addition of hydroxide anion to Sp, **1**. Addition of hydroxide to the C6 carbonyl of Sp is predicted to be endothermic by 21.8 kcal/mol, however, at this level of theory a transition state has not been identified. Proton transfer and cleavage of the C6-N1 bond should lead to the formation of the 4-carboxy-guanidinohydantoin anion, **12**. At the level of theory used in this study, a loosely bound complex of carbon dioxide and Gh anion was identified. This structure had a C6-C4 bond length of 1.64Å and was 23.8 kcal/mol lower in energy than intermediate **11**. The forward barrier height for formation of this product is 28.3 kcal/mol. Decarboxylation of **12** to form the Gh anion, **13**, is predicted to be endothermic by 19.7 kcal/mol with a forward barrier height of 29.5 kcal/mol. Our calculations suggest that a kinetically more likely pathway is for the Sp diol anion, **11**, to undergo coupled proton transfer and decarboxylation to yield the Gh anion, **13,** directly. This reaction is exothermic by 4.1 kcal/mol and has a forward barrier height of 25.6 kcal/mol when modeled with one catalytic molecule of water. Protonation of **13** at the C5 oxygen is endothermic by 1.4 kcal/mol and yields Gh enol, **10**, which then undergoes enol-keto tautomerization to form Gh, **7,** as described previously.

The data suggests that the kinetically and thermodynamically favored mechanism along Pathway A likely proceeds via proton-assisted water addition to the C6 carbonyl group to yield the *gem*-diol intermediate followed by proton-transfer and decarboxylation to form the Gh enol, **5**. Tautomerization of the enol, **5**, yields the protonated Gh species, **6**. Base-assisted conversion of Sp, **1**, to Gh, **2**, via an anion intermediate along Pathway A is predicted to be thermodynamically unfavorable.

Pathway B (Scheme 3)—The energetics for formation of Gh, **7**, from Sp, **1**, via a carbamate intermediate were evaluated for neutral, protonated and deprotonated intermediates using the procedures described for Pathway A (Scheme 3 and Figure 5). Under neutral conditions, concurrent addition of water and cleavage of the C-6-C4 bond to yield the carbamate intermediate, **14**, is predicted to be endothermic by 22.9 kcal/mol with a forward barrier height modeled with one reactive and one catalytic molecule of water of 51.2 kcal/mol. Protonation of Sp at the N1 nitrogen reduces the forward barrier height for this reaction to 34.0 kcal/mol (**2/14N1H$^+$ TS**). Deprotonation of the **14N1H$^+$** cation intermediate is exothermic by 1.1 kcal/mol. Enol-keto tautomerization of the carbamate enol intermediate, **14**, leads to formation of **15** and is exothermic by 31.4 kcal/mol with a forward barrier height modeled with two explicit water molecules of 27.6 kcal/mol. Coupled proton-transfer and decarboxylation of **15** yielding Gh, **7**, is predicted to be endothermic by 3.0 kcal/mol with a forward barrier height of 14.3 kcal/mol. Alternatively, proton-transfer and decarboxylation could take place from the carbamate enol, **14**, producing the Gh enol, **10,** which then tautomerizes to form Gh, **7**. The forward barrier height for decarboxylation of the carbamate enol, **14**, is only 15.5 kcal/mol; suggesting that this reaction is kinetically preferred to the enol-keto tautomerization **(14/15 TS)**. Deprotonation of Sp, **1**, followed by addition of water to the C6 carbonyl, leads to the formation of the Sp diol anion, **11**, shown in Figure 4. This reaction is endothermic by 21.8 kcal/mol and the intermediate has C4-C6 and C6-N1 bond lengths of Å and 1.49 Å, respectively. At the level of theory used in this study, we were not able to identify either an unbound carbamate anion intermediate or a transition state for complete cleavage of the C4-C6 bond suggesting that, under basic conditions, ring opening and decarboxylation probably proceeds via cleavage of the C6-N1 bond, as described previously for Pathway A.

The data suggest that Pathway A would be thermodynamically preferred over Pathway B as the predicted relative energies of the gem diol and C4-carboxy-Gh intermediates along Pathway A are approximately 8 to 12 kcal/mol lower in energy than the carbamate enol intermediates along Pathway B. Under protonated and neutral conditions, Pathway A may also be kinetically preferred over Pathway B as the forward barrier heights for the initial hydration reactions along Pathway A are 19.5 and 8.2 kcal/mol lower than the coordinated hydration and ring opening reactions along Pathway B.

Pathway C (Scheme 4)—The energetics for formation of Gh, **7**, from Sp, **1**, via water-assisted proton transfer and ring opening to an isocyanate enol intermediate, **16**, were also evaluated. The structures and relative energies of all reactants, intermediates and products are provided in Scheme 4 and Figure 6. Formation of the isocyanate enol intermediate, **16**, from Sp, **1**, is predicted to be endothermic by 33.9 kcal/mol. The energetics of formation of Gh, **7**, from the isocyanate enol intermediate, **16**, have been described previously(23) and are summarized here for clarity. The kinetically favored mechanism was predicted to be hydration of **16** to form the carbamate enol intermediate **17** followed by decarboxylation to Gh enol, **18**, and subsequent tautomerization to form Gh, **7**.

Under neutral conditions, the forward barrier height for the initial step along Pathway C, ring opening of Sp, **1**, to form the isocyanate enol, **16**, is approximately 10 to 18 kcal/mol lower in energy than the initial steps along Pathways A and B. However, the intermediates along Pathway C are at least 10 kcal/mol higher in energy than those along Pathways A and B making Pathway C thermodynamically less favorable. The protonated variant of Pathway A remains the kinetically preferred pathway.

Pathway D (Scheme 5)—The energetics for formation of Gh, **7**, from Sp, **1**, via reversion to 5-OH-OG (Scheme 5) and then acid-catalyzed hydration of the carbonyl at C-6 and decarboxylation to Gh were investigated in our previous study(23) and are summarized in Figure 7. Formation of 5-OH-OG, **24**, from Sp is predicted to be endothermic by 22.8 kcal/

mol. The forward barrier heights for formation of the isocyanate intermediate, **16**, and the 5-OH-OG zwitterion intermediate, **22**, are 33.1 and 33.9 kcal/mol, respectively, approximately 10 to 20 kcal/mol lower than the barrier height predicted for the initial steps along Pathways A and B. However, the isocyanate and 5-OH-OG intermediates initially formed along Pathway D are at least 10 kcal/mol higher in energy than those along Pathways A making Pathway D thermodynamically less favorable. The kinetically preferred pathway remains the protonated variant of Pathway A.

Conclusions

Spiroiminodihydantoin and guanidinohydantoin are highly mutagenic lesions found in DNA subjected to oxidative stress. Their quantification in cellular DNA samples is therefore of immediate interest. The present experimental studies highlight the fact that care must be exercised in the manipulation and storage of DNA samples containing Sp because prolonged incubation at low pH will result in conversion of Sp to Gh.

Quantitative analysis of the conversion indicates that Sp is converted to Gh at pH 1.5 with a half-life of approximately one week. The reaction slows dramatically if the pH is maintained above 4. Thus, while Sp to Gh conversion also occurs in oligodeoxynucleotides at pH 3.5, the reaction is negligible at pH 5.3 where nuclease digestion might be conducted for trace analysis of lesions in oxidatively damaged DNA. Nevertheless, HPLC separation conditions often call for the use of formic acid or trifluoroacetic acid-containing solvent systems, and these conditions could be detrimental to accurate measurement of the relative amounts of Sp compared to Gh.

Four pathways were evaluated for formation of Gh from Sp. Pathways A, B and C all involve hydration of the C6 carbonyl, ring opening and decarboxylation. Pathways A and C differ by the order of hydration and cleavage of the C4-C6 bond. Pathway B considers the energetics of concurrent hydration at C6 and cleavage of the C6-N1 bond. In Pathway D, Sp reverts to 5-OH-OG prior to hydration, ring opening, decarboxylation. The computational data suggest that formation of Gh from Sp most likely proceeds via proton-assisted hydration of the C-6 carbonyl group to yield the *gem*-diol intermediate followed by proton-transfer and decarboxylation to form the Gh enol (Figure 4, Pathway A). The barrier height for the initial step along this pathway (2/3TS) is at least 20 kcal/mol lower than those for the other three pathways. In addition, the key intermediates along this pathway, the Sp gem-diol (**3** and **8**) and the C4-carboxy-Gh (**4** and **9**) are thermodynamically favored over intermediates along Pathways B, C and D by 7.6 to 19.4 kcal/mol. Tautomerization of the Gh enol formed via any of the four pathways results in formation of Gh. Since the calculations are in an achiral environment, both the R and S enantiomers yield the same energetics along the reaction path. However, in a chiral environment, e.g. within a DNA oligomer, the two enantiomers could have different reactivities.

Supplementary Material

Refer to Web version on PubMed Central for supplementary material.

Acknowledgments

This work was supported by grants from the National Science Foundation (CHE 0512144 to HBS, CHE 0809483 to CJB and REU grant CHE-0649039). The authors thank C&IT, ISC, and the Department of Chemistry at Wayne State University for computer time.

References

1. Henderson PT, Delaney JC, Gu F, Tannenbaum SR, Essigmann JM. Oxidation of 7,8-dihydro-8-oxoguanine affords lesions that are potent sources of replication errors in vivo. Biochemistry 2002;41:914–921. [PubMed: 11790114]
2. Henderson PT, Delaney JC, Muller JG, Neeley WL, Tannenbaum SR, Burrows CJ, Essigmann JM. The hydantoin lesions formed from oxidation of 7,8-dihydro-8-oxoguanine are potent sources of replication errors in vivo. Biochemistry 2003;42:9257–9262. [PubMed: 12899611]
3. Hickerson RP, Prat F, Muller JG, Foote CS, Burrows CJ. Sequence and stacking dependence of 8-oxoguanine oxidation: Comparison of one-electron vs singlet oxygen mechanisms. J. Am. Chem. Soc 1999;121:9423–9428.
4. Cadet J, Douki T, Gasparutto D, Ravanat JL. Oxidative damage to DNA: formation, measurement and biochemical features. Mutat. Res 2003;531:5–23. [PubMed: 14637244]
5. Hah SS, Kim HM, Sumbad RA, Henderson PT. Hydantoin derivative formation from oxidation of 7,8-dihydro-8-oxo-2'-deoxyguanosine (8-oxodG) and incorporation of C-14-labeled 8-oxodG into the DNA of human breast cancer cells. BioMed. Chem. Lett 2005;15:3627–3631.
6. Hosford ME, Muller JG, Burrows CJ. Spermine participates in oxidative damage of guanosine and 8-oxoguanosine leading to deoxyribosylurea formation. J. Am. Chem. Soc 2004;126:9540–9541. [PubMed: 15291548]
7. Luo WC, Muller JG, Rachlin EM, Burrows CJ. Characterization of spiroiminodihydantoin as a product of one-electron oxidation of 8-oxo-7,8-dihydroguanosine. Org. Lett 2000;2:613–616. [PubMed: 10814391]
8. Luo WC, Muller JG, Burrows CJ. The pH-dependent role of superoxide in riboflavin-catalyzed photooxidation of 8-oxo-7,8-dihydroguanosine. Org. Lett 2001;3:2801–2804. [PubMed: 11529760]
9. Luo WC, Muller JG, Rachlin EM, Burrows CJ. Characterization of hydantoin products from one-electron oxidation of 8-oxo-7,8-dihydroguanosine in a nucleoside model. Chem. Res. Toxicol 2001;14:927–938. [PubMed: 11453741]
10. McCallum JEB, Kuniyoshi CY, Foote CS. Characterization of 5-hydroxy-8-oxo-7,8-dihydroguanosine in the photosensitized oxidation of 8-oxo-7,8-dihydroguanosine and its rearrangement to spiroiminodihydantoin. J. Am. Chem. Soc 2004;126:16777–16782. [PubMed: 15612716]
11. Joffe A, Geacintov NE, Shafirovich V. DNA lesions derived from the site selective oxidation of guanine by carbonate radical anions. Chem. Res. Toxicol 2003;16:1528–1538. [PubMed: 14680366]
12. Misiaszek R, Crean C, Joffe A, Geacintov NE, Shafirovich V. Oxidative DNA damage derived from a combination of superoxide with guanine and 8-oxo-7,8-dihydroguanine radicals. Chem. Res. Toxicol 2004;17:1765–1765.
13. Misiaszek R, Crean C, Geacintov NE, Shafirovich V. Combination of nitrogen dioxide radicals with 8-oxo-7,8-dihydroguanine and guanine radicals in DNA: Oxidation and nitration end-products. J. Am. Chem. Soc 2005;127:2191–2200. [PubMed: 15713097]
14. Misiaszek R, Crean C, Joffe A, Geacintov NE, Shafirovich V. Oxidative DNA damage associated with combination of guanine and superoxide radicals and repair mechanisms via radical trapping. J. Biol. Chem 2004;279:32106–32115. [PubMed: 15152004]
15. Neeley WL, Essigmann JM. Mechanisms of formation, genotoxicity, and mutation of guanine oxidation products. Chem. Res. Toxicol 2006;19:491–505. [PubMed: 16608160]
16. Niles JC, Wishnok JS, Tannenbaum SR. Spiroiminodihydantoin is the major product of the 8-oxo-7,8-dihydroguanosine reaction with peroxynitrite in the presence of thiols and guanosine photooxidation by methylene blue. Org. Lett 2001;3:963–966. [PubMed: 11277770]
17. Niles JC, Wishnok JS, Tannenbaum SR. Spiroiminodihydantoin and guanidinohydantoin are the dominant products of 8-oxoguanosine oxidation at low fluxes of peroxynitrite: Mechanistic studies with O-18. Chem. Res. Toxicol 2004;17:1510–1519. [PubMed: 15540949]
18. Ye Y, Muller JG, Luo WC, Mayne CL, Shallop AJ, Jones RA, Burrows CJ. Formation of C-13-, N-15-, and O-18-labeled guanidinohydantoin from guanosine oxidation with singlet oxygen. Implications for structure and mechanism. J. Am. Chem. Soc 2003;125:13926–13927. [PubMed: 14611206]

19. Yu HB, Venkatarangan L, Wishnok JS, Tannenbaum SR. Quantitation of four guanine oxidation products from reaction of DNA with varying doses of peroxynitrite. Chem. Res. Toxicol 2005;18:1849–1857. [PubMed: 16359175]
20. Niles JC, Wishnok JS, Tannenbaum SR. Peroxynitrite-induced oxidation and nitration products of guanine and 8-oxoguanine: Structures and mechanisms of product formation. Nitric Oxide 2006;14:109–121. [PubMed: 16352449]
21. Niles JC, Venkatarangan LM, Wishnok JS, Tannenbaum SR. Probing the mechanism of peroxynitrite-induced oxidation of guanine and 8-oxoguanine. Chem. Res. Toxicol 2002;15:1675–1676.
22. Slade PG, Priestley ND, Sugden KD. Spiroiminodihydantoin as an Oxo-Atom Transfer Product of 8-Oxo-2'-deoxyguanosine Oxidation by Chromium (V). Org. Lett 2007;9:4411–4414. [PubMed: 17915881]
23. Munk BH, Burrows CJ, Schlegel HB. An Exploration of Mechanisms for the Transformation of 8-Oxoguanine to Guanidinohydantoin and Spiroiminodihydantoin by Density Functional Theory. J. Am. Chem. Soc 2008;130:5245–5256. [PubMed: 18355018]
24. Kornyushyna O, Berges AM, Muller JG, Burrows CJ. In vitro nucleotide misinsertion opposite the oxidized guanosine lesions spiroiminodihydantoin and guanidinohydantoin and DNA synthesis past the lesions using Escherichia coli DNA polymerase I (Klenow fragment). Biochemistry 2002;41:15304–15314. [PubMed: 12484769]
25. Yu HB, Niles JC, Wishnok JS, Tannenbaum SR. Spirodihydantoin is a minor product of 5-hydroxyisourate in urate oxidation. Org. Lett 2004;6:3417–3420. [PubMed: 15355066]
26. Poje M, Sokolicmaravic L. The mechanism for the conversion of uric-acid into uroxanate and allantoin - a new base-induced 1,2 carboxylate shift. Tetrahedron 1988;44:6723–6728.
27. Kahn K, Serfozo P, Tipton PA. Identification of the true product of the urate oxidase reaction. J. Am. Chem. Soc 1997;119:5435–5442.
28. Frisch, MJ.; Trucks, GW.; Schlegel, HB.; Scuseria, GE.; Robb, MA.; Cheeseman, JR.; Montgomery, JA., Jr.; Vreven, T.; Scalmani, G.; Kudin, KN.; Iyengar, SS.; Tomasi, J.; Barone, V.; Mennucci, B.; Cossi, M.; Rega, N.; Petersson, GA.; Nakatsuji, H.; Hada, M.; Ehara, M.; Toyota, K.; Fukuda, R.; Hasegawa, J.; Ishida, M.; Nakajima, T.; Honda, Y.; Kitao, O.; Nakai, H.; Li, X.; Hratchian, HP.; Peralta, JE.; Izmaylov, AF.; Brothers, E.; Staroverov, V.; Kobayashi, R.; Normand, J.; Burant, JC.; Millam, JM.; Klene, M.; Knox, JE.; Cross, JB.; Bakken, V.; Adamo, C.; Jaramillo, J.; Gomperts, R.; Stratmann, RE.; Yazyev, O.; Austin, AJ.; Cammi, R.; Pomelli, C.; Ochterski, JW.; Ayala, PY.; Morokuma, K.; Voth, GA.; Salvador, P.; Dannenberg, JJ.; Zakrzewski, VG.; Dapprich, S.; Daniels, AD.; Strain, MC.; Farkas, O.; Malick, DK.; Rabuck, AD.; Raghavachari, K.; Foresman, JB.; Ortiz, JV.; Cui, Q.; Baboul, AG.; Clifford, S.; Cioslowski, J.; Stefanov, BB.; Liu, G.; Liashenko, A.; Piskorz, P.; Komaromi, I.; Martin, RL.; Fox, DJ.; Keith, T.; Al-Laham, MA.; Peng, CY.; Nanayakkara, A.; Challacombe, M.; Chen, W.; Wong, MW.; Pople, JA. Gaussian DV. Gaussian, Inc.; Wallingford, CT: 2006.
29. Becke AD. Density functional exchange energy approximation with correct asymptotic behavior. Phys. Rev. A 1988;38:3098–3100. [PubMed: 9900728]
30. Becke AD. Density functional theory. III. The role of exact exchange. J. Chem. Phys 1993;98:5648–5652.
31. Lee C, Yang W, Parr RD. Development of the Colle-Salvetti correlation energy formula into a functional of the electron density. Phys. Rev. B 1988;37:785–789.
32. Ditchfield R, Hehre WJ, Pople JA. Self-consistent molecular-orbital methods. IX. An extended Gaussian-type basis for molecular-orbital studies of organic molecules. J. Chem. Phys 1971;54:724–728.
33. Hehre WJ, Ditchfield R, Pople JA. Self—consistent molecular orbital methods. XII. Further extensions of Gaussian—type basis sets for use in molecular Orbital studies of organic molecules. J. Chem. Phys 1972;56:2257–2261.
34. Hariharan PC, Pople JA. The influence of polarization functions on molecular orbital hydrogenation energies. Theoret. Chim. Acta 1973;28:213–222.
35. Hariharan PC, Pople JA. Accuracy of AH, equilibrium geometries by single determinant molecular orbital theory. Mol. Phys 1974;27:209–214.
36. Gordon MS. The isomers of silacyclopropane. Chem. Phys. Lett 1980;76:163–168.

37. Francl MM, Pietro WJ, Hehre WJ, Binkley JS, Gordon MS, Defrees DJ, Pople JA. Self-consistent molecular-orbital methods .23. A polarization-type basis set for 2nd-row elements. J. Chem. Phys 1982;77:3654–3665.
38. Munk BH, Burrows CJ, Schlegel HB. Exploration of mechanisms for the transformation of 8-hydroxy guanine radical to FAPyG by density functional theory. Chem. Res. Toxicol 2007;20:432–444. [PubMed: 17316026]
39. Kendall RA, Dunning TH, Harrison RJ. Electron-Affinities of the 1st-Row Atoms Revisited - Systematic Basis-Sets and Wave-Functions. J. Chem. Phys 1992;96:6796–6806.
40. Scott AP, Radom L. Harmonic vibrational frequencies: An evaluation of Hartree- Fock, Moller-Plesset, quadratic configuration interaction, density functional theory, and semiempirical scale factors. J. Phys. Chem 1996;100:16502–16513.
41. McQuarrie, DA. Statistical Thermodynamics. University Science Books; Mill Valley, CA: 1973.
42. Cucinotta CS, Ruini A, Catellani A, Stirling A. Ab initio molecular dynamics study of the keto-enol tautomerism of acetone in solution. Chemphyschem 2006;7:1229–1234. [PubMed: 16683282]
43. Lee D, Kim CK, Lee BS, Lee I, Lee BC. A theoretical study on ketoenol tautomerization involving simple carbonyl derivatives. J. Comput. Chem 1997;18:56–69.
44. Capon B, Zucco C. Simple Enols .2. Kinetics and Mechanism of the Ketonization of Vinyl Alcohol. J. Am. Chem. Soc 1982;104:7567–7572.
45. Verdolino V, Cammi R, Munk BH, Schlegel HB. Calculation of pKa values of nucleobases and the guanine oxidation products guanidinohydantoin and spiroiminodihydantoin using density functional theory and the ppolarizable continuum model. J. Phys. Chem. B. 2008 in press. (DOI: 10.1021/jp8068877).
46. Cho BP. Structure of oxidatively damaged nucleic-acid adducts - pH-dependence of the C-13 NMR-spectra of 8-oxoguanosine and 8-oxoadenosine. Magn. Reson. Chem 1993;31:1048–1053.
47. Eckert F, Klamt A. Accurate prediction of basicity in aqueous solution with COSMO-RS. J. Comput. Chem 2006;27:11–19. [PubMed: 16235262]

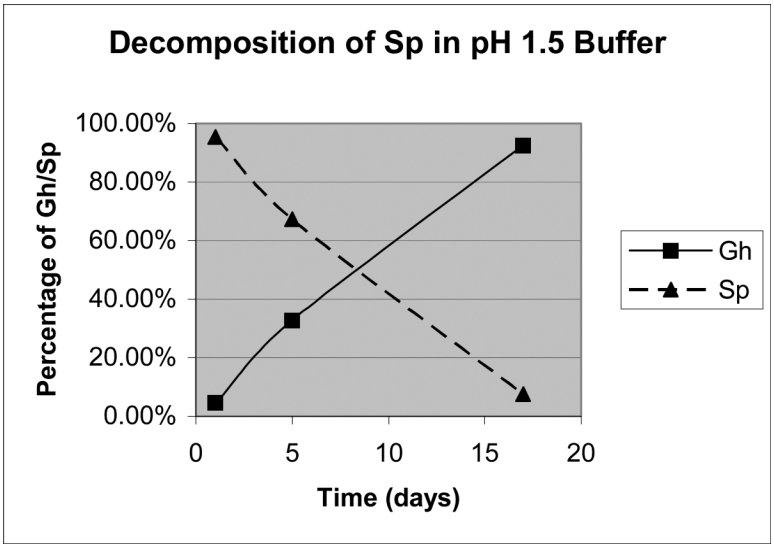

Figure 1.
The percentages of Gh and Sp at different incubation times in pH 1.5 buffer, corrected for relative ionization as analyzed by ESI-MS.

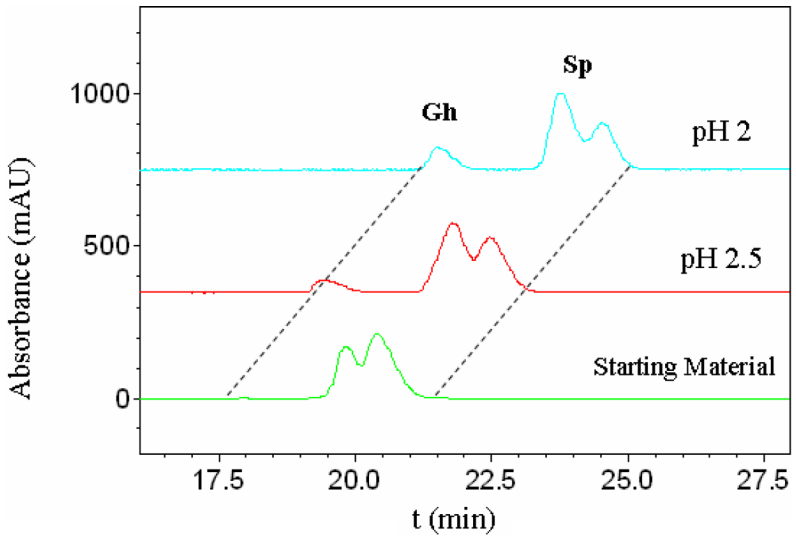

Figure 2.

HPLC analysis of Sp nucleoside diastereomers converting to Gh after being incubated at pH 2 or 2.5 for 3 days. Identities of Gh and Sp were confirmed by ESI-MS and comparison to authentic samples.

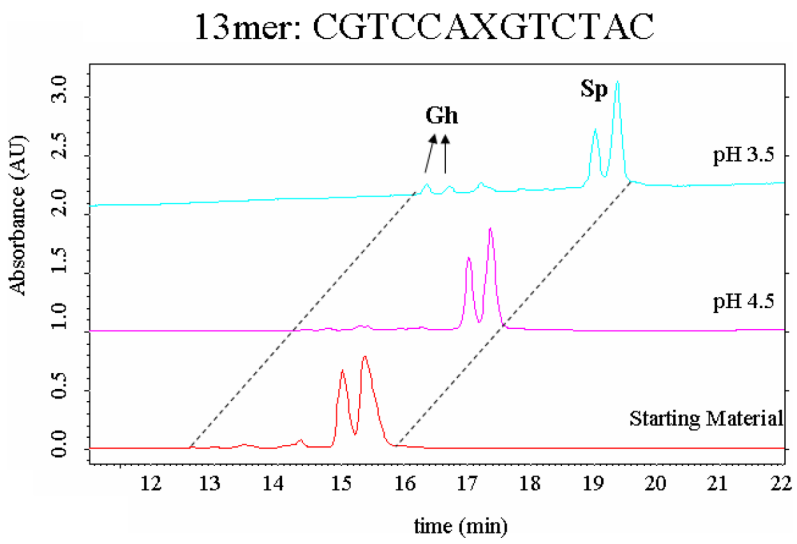

Figure 3.
HPLC analysis of an Sp-containing oligomer (X = Sp) converting to Gh after overnight incubation at pH 3.5 vs. 4.5.

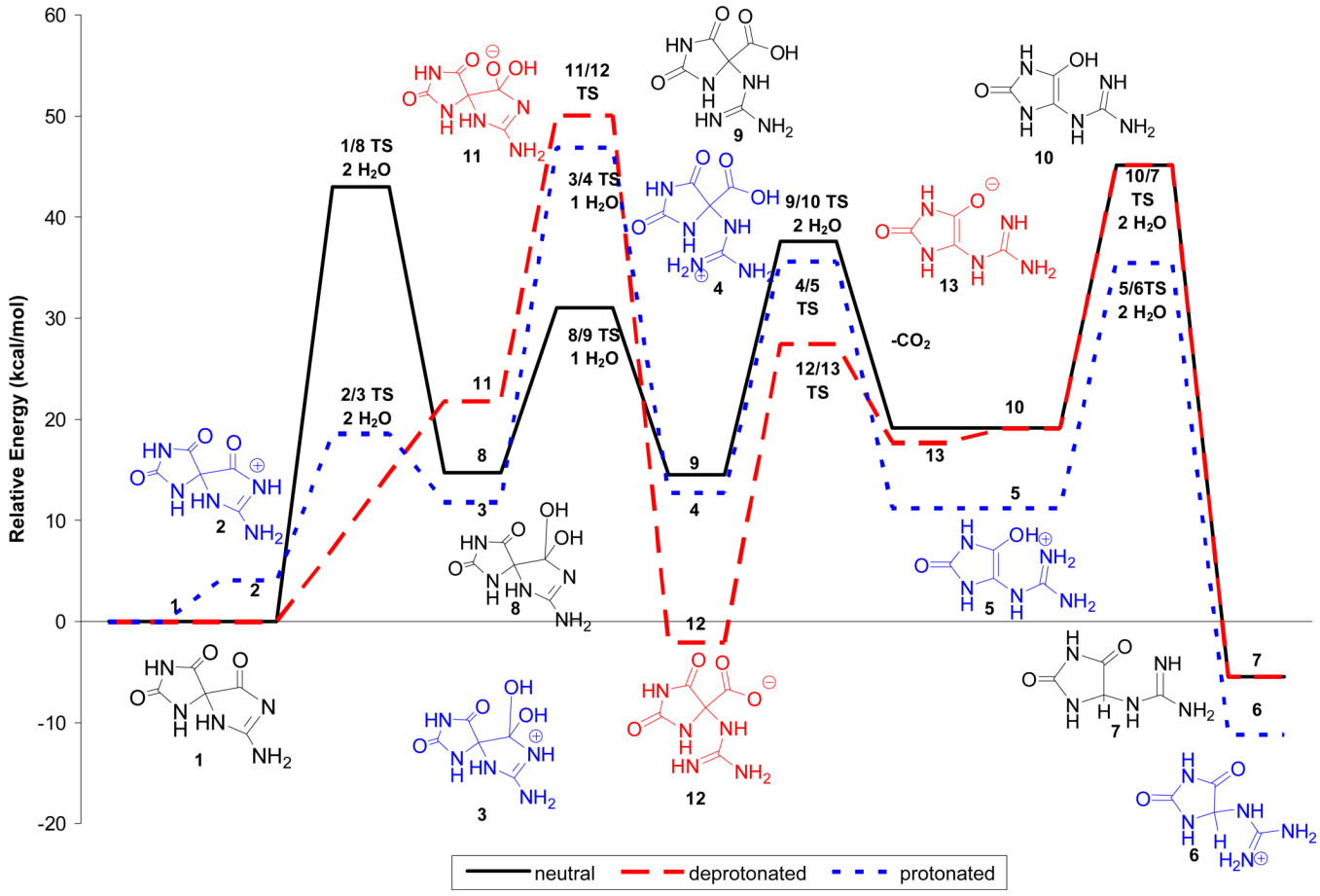

Figure 4.

Relative energies in solution of Pathway A under neutral (solid black line), basic (red dashed line), and acidic (blue dotted line) conditions for formation of Gh, **7**, from Sp, **1** calculated at IEF-PCM/B3LYP/aug-cc-pVTZ//B3LYP/6-31+G(d,p).

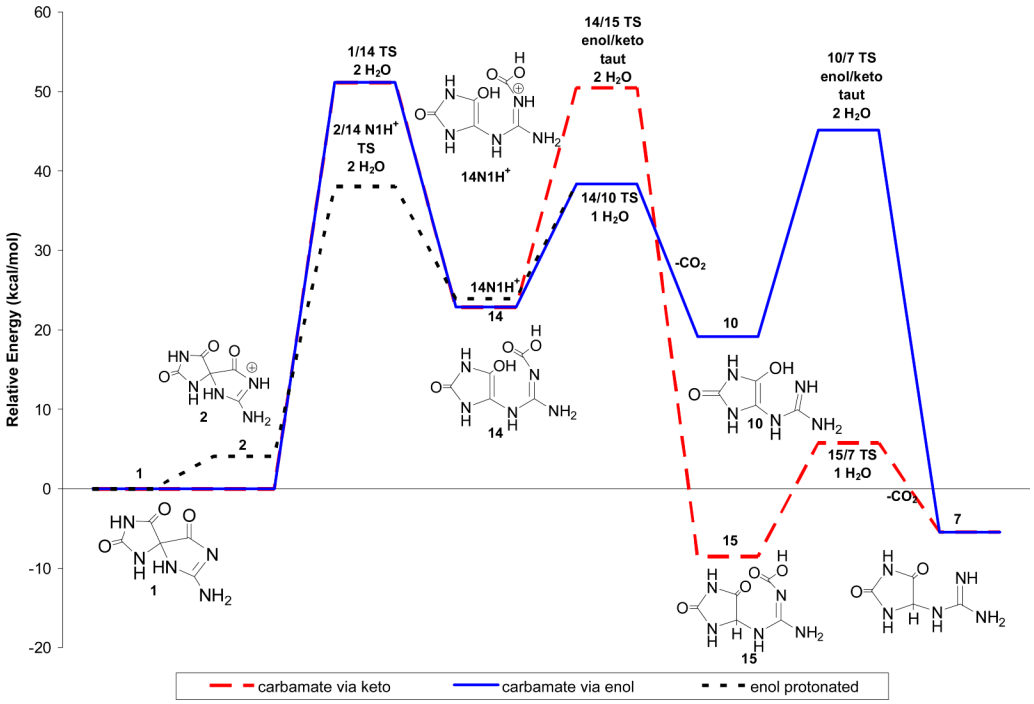

Figure 5.

Relative energies in solution of Pathway B via the enol (solid blue line) or ketone (red dashed line) for formation of Gh, **7**, from Sp, **1** calculated at IEF-PCM/B3LYP/aug-cc-pVTZ//B3LYP/6-31+G(d,p).

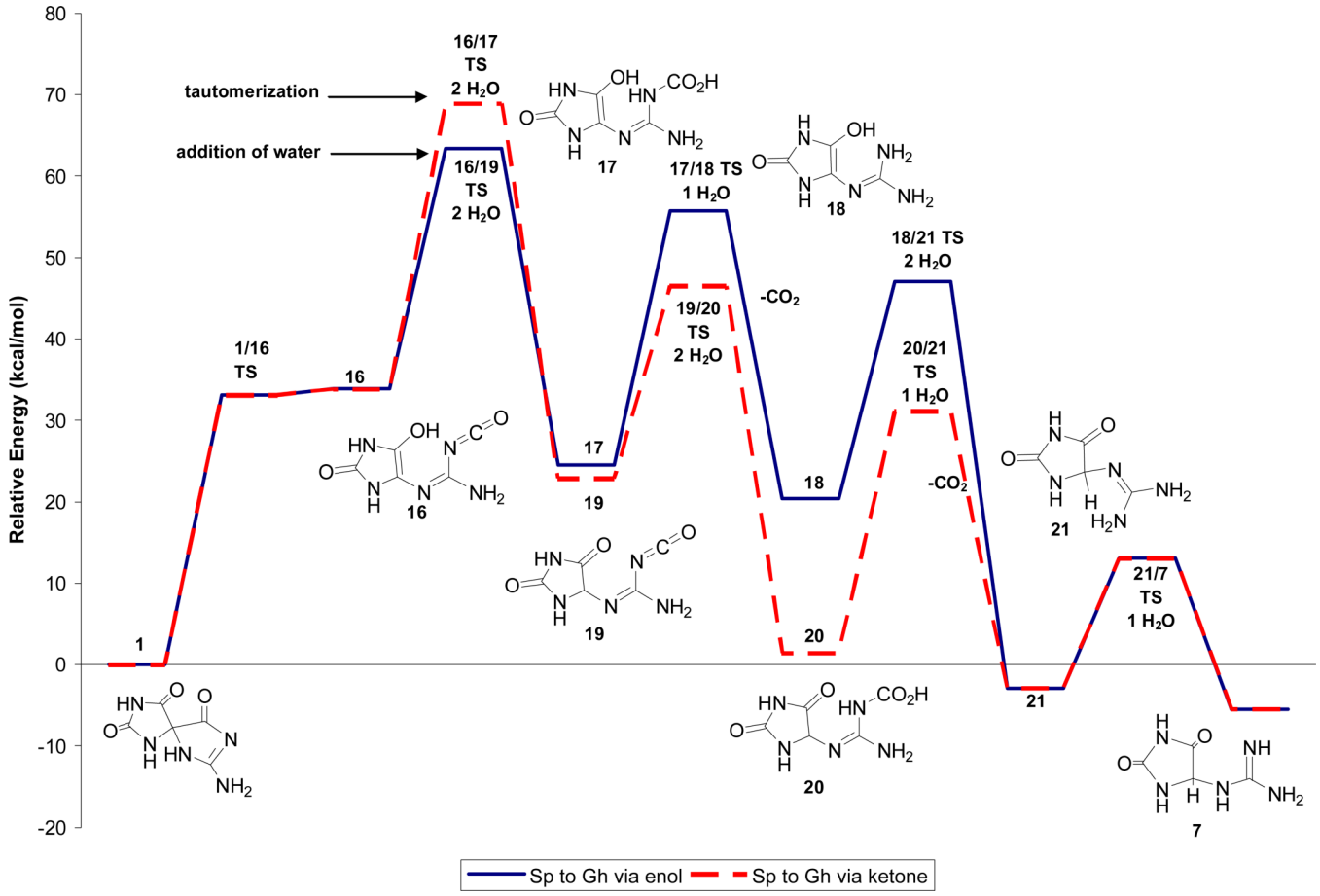

Figure 6.

Relative energies in solution of Pathway C via the enol (solid blue line) or ketone (red dashed line) for formation of Gh, **7**, from Sp, **1** calculated at IEF-PCM/B3LYP/aug-cc-pVTZ//B3LYP/6-31+G(d,p).

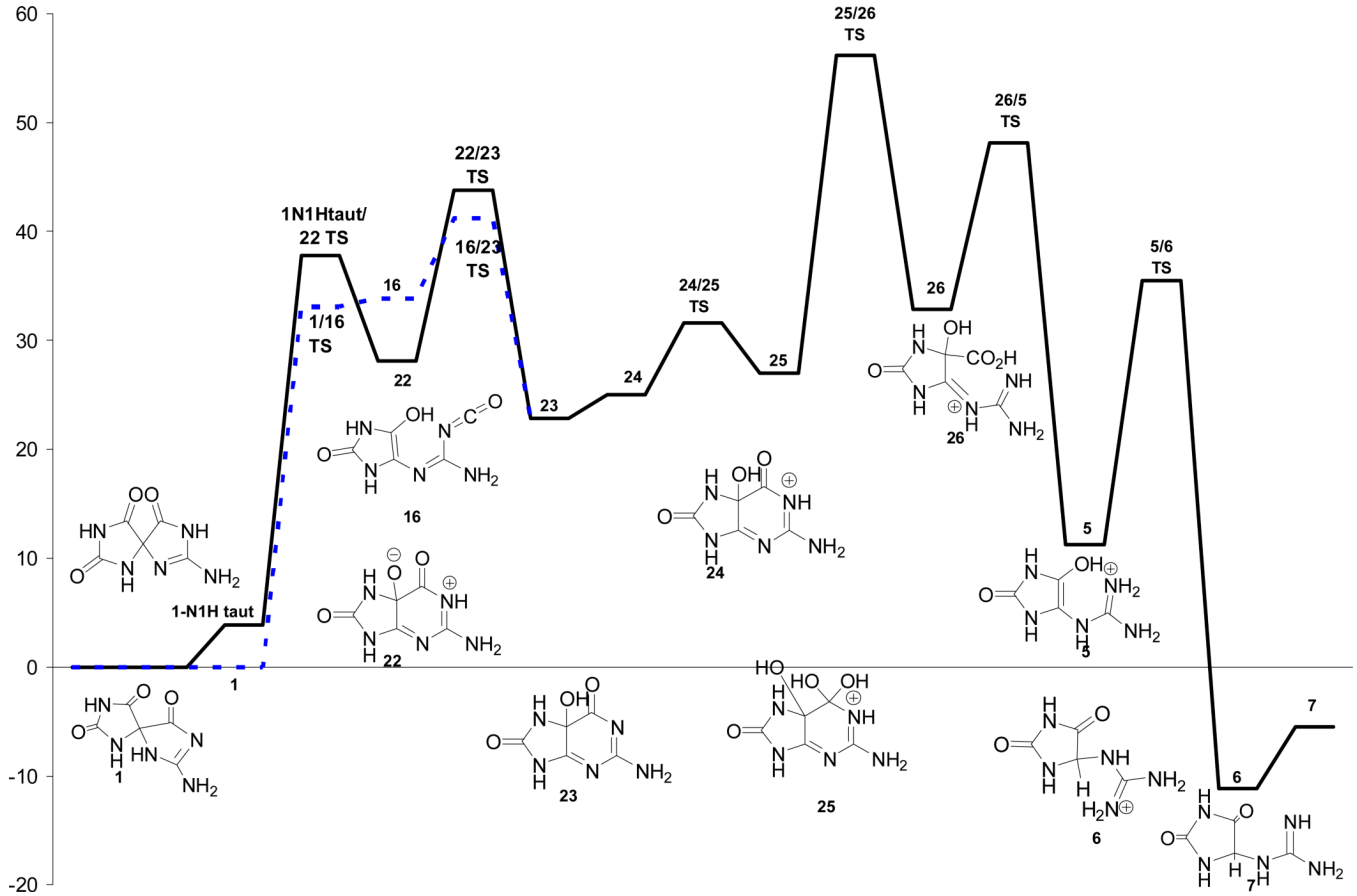

Figure 7.

Relative energies in solution of Pathway D via initial reversion of Sp, **1**, to 5-OH-OG, **23**, and then acid-catalyzed formation of Gh, **7**, via the 5-carboxy-Gh intermediate, **26**, calculated at IEF-PCM/B3LYP/aug-cc-pVTZ//B3LYP/6-31+G(d,p).

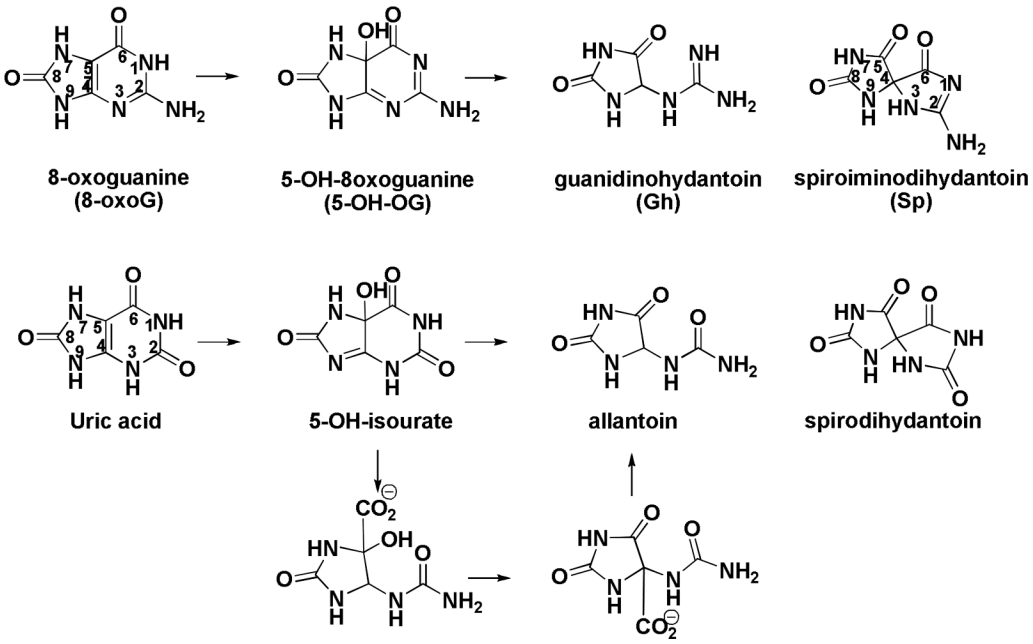

Scheme 1.

Comparison of pathways for conversion of 8-oxoG to Gh, **7**, and Sp, **1**, and for conversion of uric acid to allantoin and spirodihydantoin.

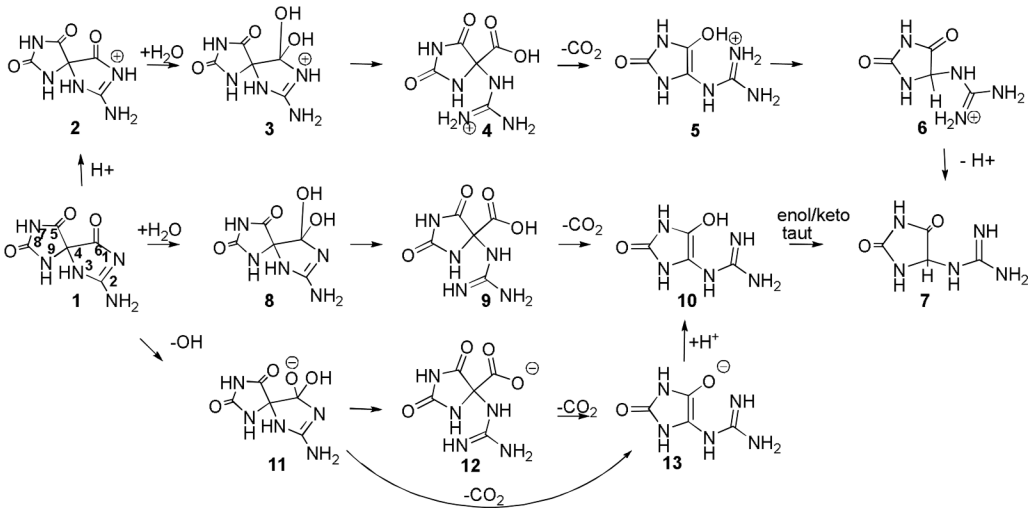

Scheme 2.
Possible pathway for conversion of Sp, **1**, to Gh, **7**, via a gem diol intermediate (Pathway A).

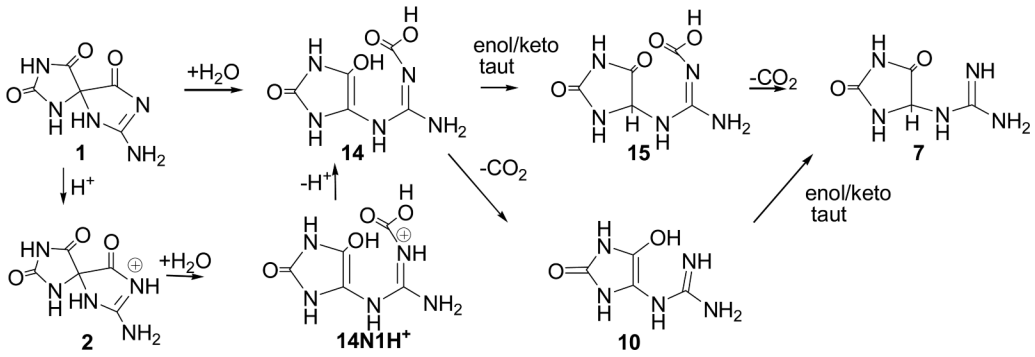

Scheme 3.

Possible pathways for conversion of Sp, **1**, to Gh, **7**, via carbamate intermediate (Pathway B)

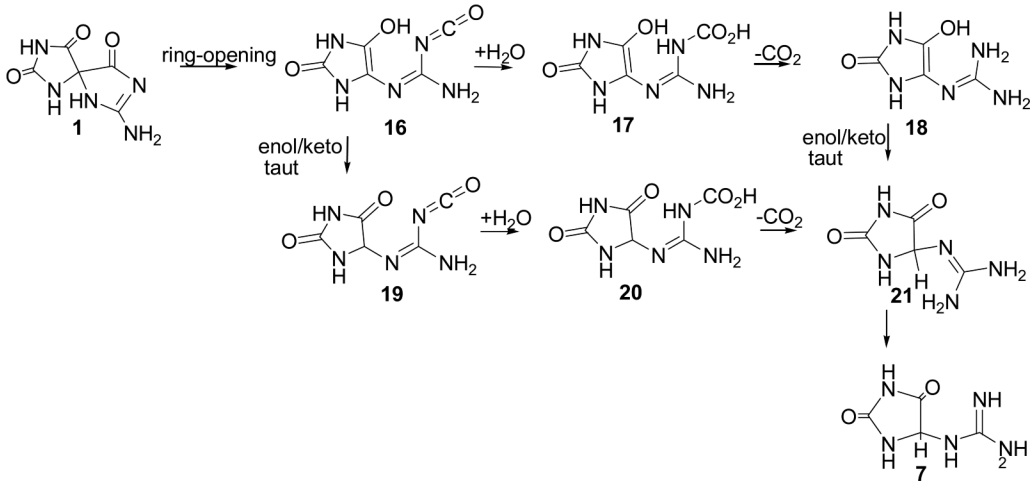

Scheme 4.

Possible pathways for conversion of Sp, **1**, to Gh, **7**, via ring opening to isocyanate intermediate (Pathway C)

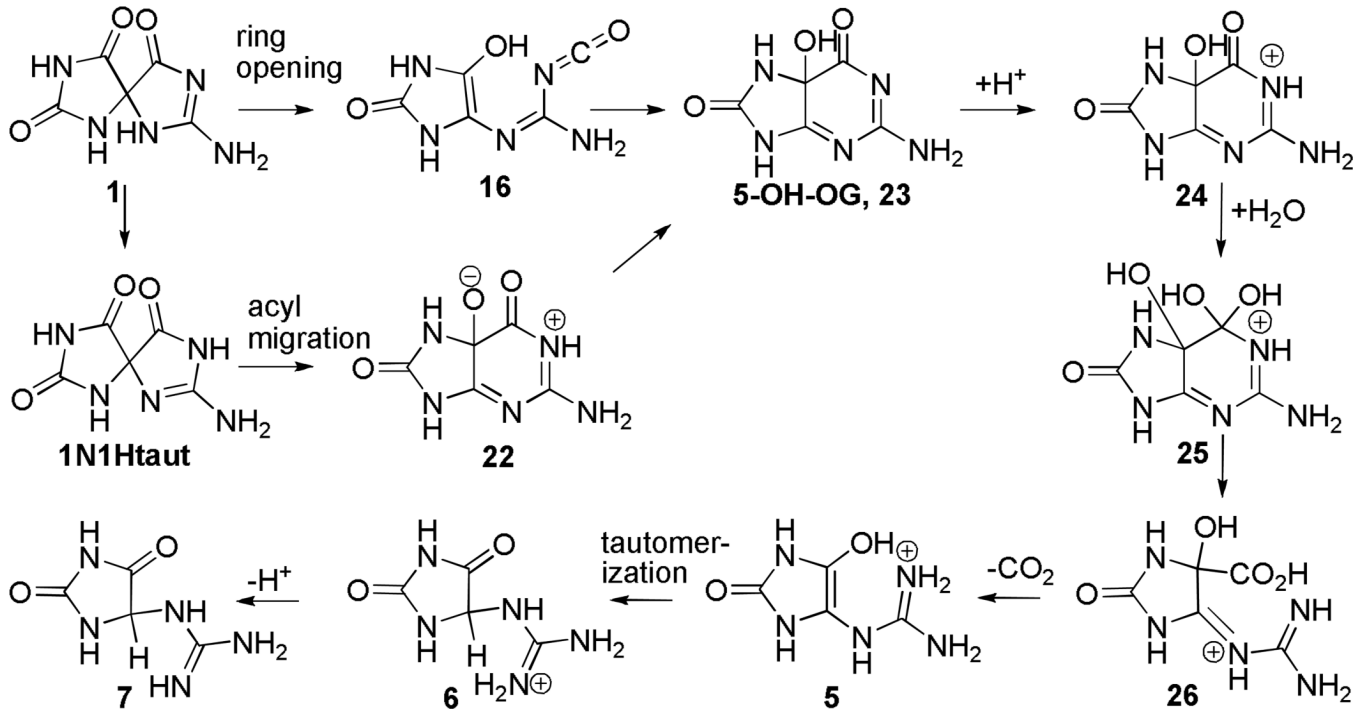

Scheme 5.
Possible pathways for conversion of Sp, **1**, to Gh, **7**, via 5-OHOG, **23**, (Pathway D)

Table 1

Relative energies of adducts for conversion of Sp, **1**, to Gh, **7**.

Summary of Energetics	Schemes 2-4 Structure No.	E + ZPE + ΔH_{298} + ΔG_{solv} (kcal/mol)
Sp + CH^+ + 3 H_2O + CH_3S^-	**1**	0.0
Sp-N1Htaut + CH^+ + 3 H_2O + CH_3S^-	**1-N1H taut**	3.9
Sp-N1HN3H imine + CH^+ + 3 H_2O + CH_3S^-	**1-N1HN3H imine**	1.9
Sp-TS-Sp diol + CH^+ + 1 H_2O + CH_3S^-	**1/8 TS**	43.0
Sp-TS-carbamate N3H enol + CH^+ + 1 H_2O + CH_3S^-	**1/14 TS**	51.2
Sp-TS-isocyanate enol + CH^+ + 1 H_2O + CH_3S^-	**1/16 TS**	33.1
Sp-C5OH^+ + C + 3 H_2O + CH_3S^-	**2-C5OH taut**	27.5
Sp-$N1H^+$ + C + 3 H_2O + CH_3S^-	**2**	4.1
Sp-C6OH^+ + C + 3 H_2O + CH_3S^-	**2-C6OH taut**	17.9
Sp-C6OH^+ TS Sp diol $N1H^+$ + C + 2 H_2O + CH_3S^-	**2-C6OHtaut /3 TS**	43.1
Sp-$N1H^+$ TS carbamate enol $N1H^+$ + C + 1 H_2O + CH_3S^-	**2N1H^+/14N1H^+ TS**	38.1
Sp-N1HH^+TS-Sp diol-$N1H^+$ + C + 1 H_2O + CH_3S^-	**2/3 TS**	18.6
Sp diol-$N1H^+$ + C + 2 H_2O + CH_3S^-	**3**	11.8
Sp diol-$N1H^+$-TS-imidazolidine C4 carboxylic acid-$N1H^+$ + C + 1 H_2O + CH_3S^-	**3/4 TS**	46.9
Sp diol-$N1H^+$-(ring opening) TS-imidazolidine C4 carboxylic acid-C6OH^+ + C + 2 H_2O + CH_3S^-	**3/4C6OH^+ TS**	48.9
C4-carboxy-Gh $N1H^+$ + C + 2 H_2O + CH_3S^-	**4**	12.8
C4-carboxy-Gh $N1H^+$ TS Gh enol cation + C + 2 H_2O + CH_3S^-	**4/5TS**	35.7
C4-carboxy-Gh C5OH^+ + C + 2 H_2O + CH_3S^-	**4C5OH^+ TS**	42.3
Gh enol $N1H^+$ + C + 2 H_2O + CH_3S^- + CO_2	**5**	11.2
Gh enol $N1H^+$-TS-Gh keto $N1H^+$ + C + CH_3S^- + CO_2	**5/6 TS**	35.5
Gh keto $N1H^+$ + C + 2 H_2O + CH_3S^- + CO_2	**6**	-11.2
Gh + CH^+ + 2 H_2O + CH_3S^- + CO_2	**7**	-5.5
Sp diol + CH^+ + 2 H_2O + CH_3S^-	**8**	14.7
Sp diol-TS-C4-carboxy-Gh + CH^+ + 2 H_2O + CH_3S^-	**8/9 TS**	31.0
C4-carboxy-Gh + CH^+ + 2 H_2O + CH_3S^-	**9**	14.5
C4-carboxy-Gh-TS-Gh enol + CH^+ + CH_3S^-	**9/10 TS**	37.6
Gh enol + CH^+ + 2 H_2O + CH_3S^- + CO_2	**10**	19.1
Gh enol-TS-Gh + CH^+ + CH_3S^- + CO_2	**10/7 TS**	45.2
SpC6diol anion + CH^+ + 2 H_2O + CH_3SH	**11**	21.8
SpC6diol anion TS Gh anion + CH^+ + 1 H_2O + CH_3SH	**11/13 TS**	47.4
C4-carboxy-Gh anion + CH^+ + 2 H_2O + CH_3SH	**12**	-2.0
C4-carboxy-Gh anion-TS-Gh anion + CH^+ + 2 H_2O + CH_3SH	**12/13 TS**	27.5
Gh enol anion + CH^+ + 2 H_2O + CH_3S^- + CO_2	**13**	17.7

Summary of Energetics	**Schemes 2-4 Structure No.**	**E + ZPE + ΔH_{298} + ΔG_{solv} (kcal/mol)**
Carbamate N3H enol + CH^+ + 2 H_2O + CH_3S^-	**14**	22.9
Carbamate N3H enol-TS-Gh N3H enol + CH^+ + 2 H_2O + CH_3S^-	**14/10 TS**	38.4
Carbamate N3H enol/keto + CH^+ + CH_3S^-	**14/15 TS**	50.5
Carbamate N1HN3H enol cation + C + 2 H_2O + CH_3S^-	**14N1H$^+$**	24.0
Carbamate N3H ketone + CH^+ + 2 H_2O + CH_3S^-	**15**	-8.5
Carbamate N3H ketone-TS-Gh + CH^+ + 1 H_2O + CH_3S^-	**15/7 TS**	5.8
Isocyanate enol + CH^+ + 3 H_2O + CH_3S^-	**16**	33.9
Isocyanate enol-TS-carbamate N1H enol + CH^+ + 1 H_2O + CH_3S^-	**16/17 TS**	63.4
Isocyanate enol-keto tautomerization + CH^+ + 1 H_2O + CH_3S^-	**16/19 TS**	68.9
Imidazolidone carbamate N1H enol + CH^+ + 2 H_2O + CH_3S^-	**17**	24.5
Imidazolidone carbamate N1H enol-TS-Gh enol + CH^+ + 1 H_2O + CH_3S^-	**17/18 TS**	55.7
Gh enol + CH^+ + 2 H_2O + CH_3S^- + CO_2	**18**	20.4
Gh-enol-ketone TS + CH^+ + CH_3S^- + CO_2	**18/21 TS**	47.0
Isocyanate ketone + CH^+ + 3 H_2O + CH_3S^-	**19**	22.9
Isocyanate keto-TS-carbamate N1H keto + CH^+ + 1 H_2O + CH_3S^-	**19/20 TS**	46.5
Imidazolidone carbamate N1H ketone + CH^+ + 2 H_2O + CH_3S^-	**20**	1.4
Imidazolidone carbamate N1H ketone-TS-Gh taut + CH^+ + H_2O + CH_3S^-	**20/21 TS**	31.1
Gh N1H2 taut + CH^+ + 2 H_2O + CH_3S^- + CO_2	**21**	-2.9
Gh N1H2 taut-TS-Gh + CH^+ + H_2O + CH_3S^- + CO_2	**21/7 TS**	13.1